Supplementary information

Death Induced by CD95 or CD95 Ligand Elimination

Abbas Hadji, Paolo Ceppi, Andrea E. Murmann, Sonia Brockway, Abhinandan Pattanayak, Bhavneet Bhinder, Annika Hau, Shirley De Chant, Vamsi Parimi, Piotre Kolesza, JoAnne Richards, Navdeep Chandel, Hakim Djaballah, and Marcus E. Peter

Supplementary Information
This file contains Supplementary Figures S1-S10 with legends, Supplementary Tables S1-S5, Supplementary Results, Supplementary Discussion, and Supplementary Methods.

SUPPLEMENTARY FIGURES

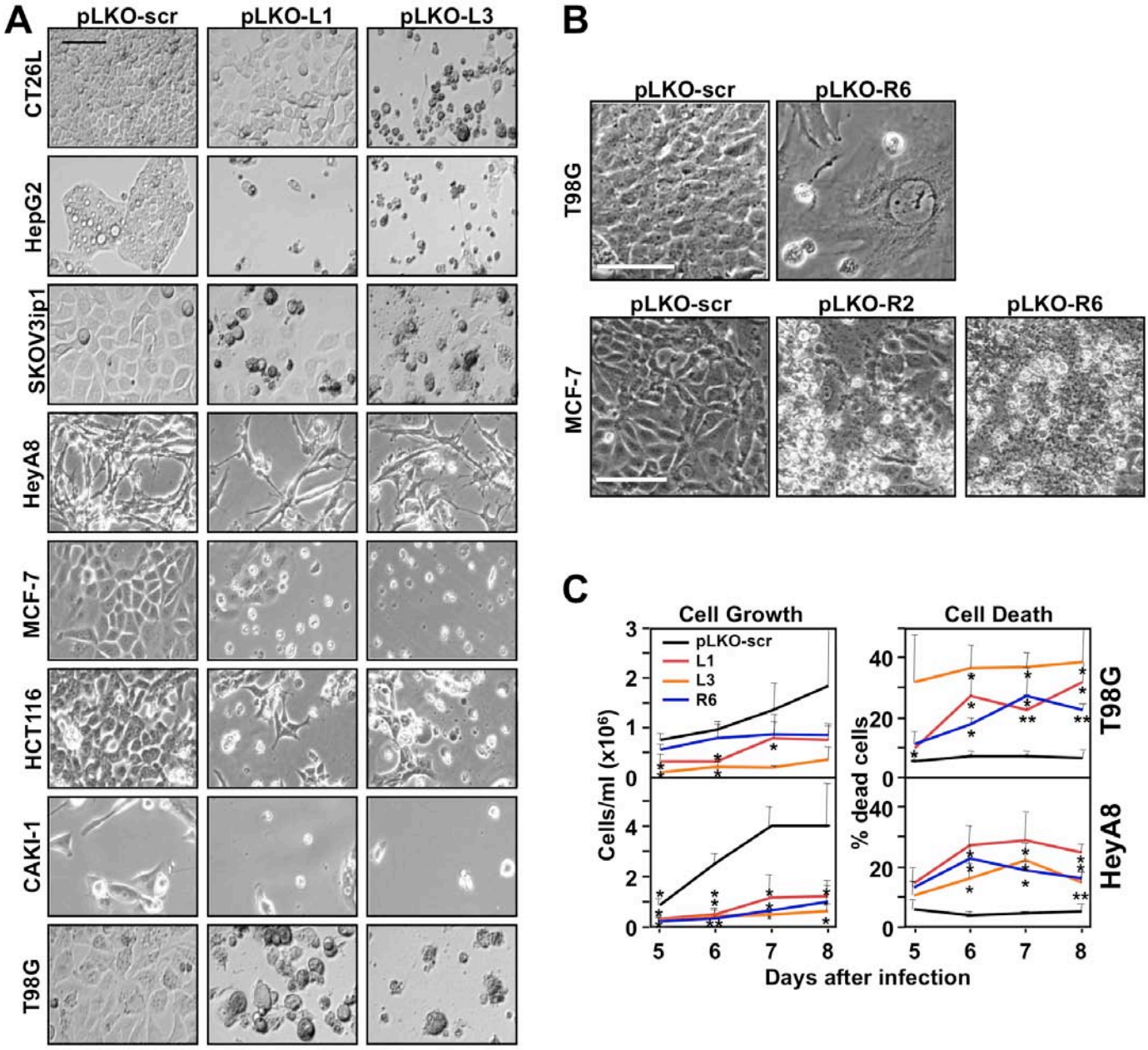

Figure S1. Characterization of CD95 and CD95L Knockdown Cells, Related to Figure 1. (A) Phase contrast images of 8 cell lines 9 days after infection with shRNA lentiviruses pLKO-L1, L3, or a control virus carrying a scrambled shRNA (pLKO-scr). To eliminate uninfected cells, puromycin was added 2 days after infection for 2 days. Scale bar = 100 μm. **(B)** Phase contrast images of T98G cells 13 days after infection and MCF-7 cells 8 days after infection with lentiviral shRNAs targeting CD95 (R2 or R6). Scale bar = 100 μm. **(C)** Quantification of cell number (left) and percentage of dead cells (right) of T98G and HeyA8 cells 5-8 days after infection with shRNA lentiviruses pLKO-L1, L3, R6, or a control virus carrying a nontargeting shRNA (pLKO-scr) without addition of puromycin. P-values were calculated using *t*-test. * = $p<0.05$; ** = $p<0.001$. Data are shown are the mean + SD from triplicate cultures from one representative experiment out of three**.**

A

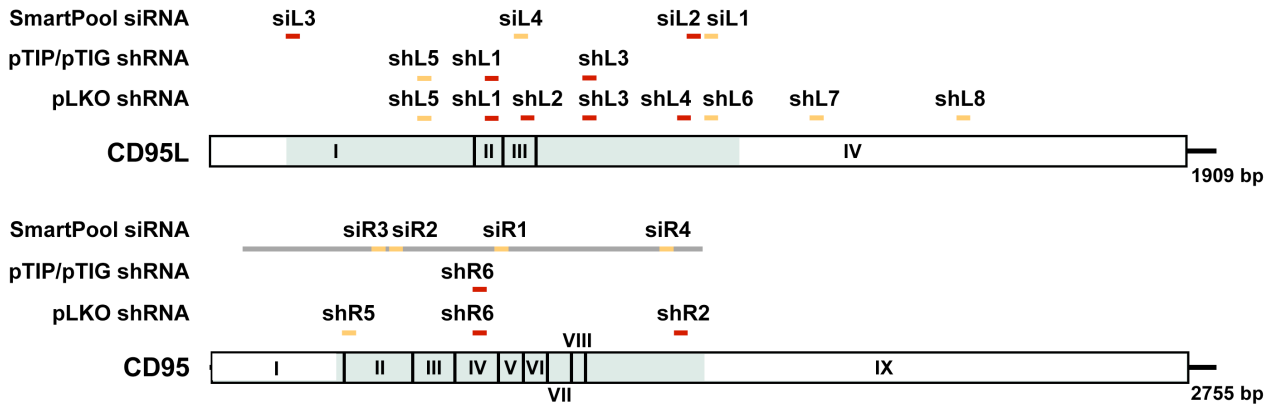

B

Gene	RefSeq	TRC#	Numbering in this study	Cell Line 1	Cell Line 2	Cell Line 3	Cell Line 4	Cell Line 5	Cell Line 6	Cell Line 7	Cell Line 8	Cell Line 9	Cell Line 10	Cell Line 11	Cell Line 12	# of cell lines killed
FAS	NM_000043	TRCN0000038696	shR6	No	Yes	Yes	No	Yes	Yes	Yes	Yes	Yes	Yes	Yes	Yes	10
FAS	NM_000043	TRCN0000038697	shR7	No	No	No	No	Yes	Yes	Yes	Yes	Yes	Yes	Yes	Yes	8
FAS	NM_000043	TRCN0000038695	shR5	No	No	No	No	Yes	Yes	No	Yes	Yes	Yes	Yes	Yes	7
FAS	NM_000043	TRCN0000038698	shR8	No	No	No	No	No	Yes	No	Yes	Yes	No	No	No	3
				No	**No**	**No**	**No**	**Yes**	**Yes**	**No**	**Yes**	**Yes**	**Yes**	**Yes**	**Yes**	**7**

Gene	RefSeq	TRC#		Cell Line 1	Cell Line 2	Cell Line 3	Cell Line 4	Cell Line 5	Cell Line 6	Cell Line 7	Cell Line 8	Cell Line 9	Cell Line 10	Cell Line 11	Cell Line 12	# of cell lines killed
FASLG	NM_000639	TRCN0000058998	shL1	Yes	Yes	Yes	No	Yes	Yes	Yes	Yes	Yes	Yes	Yes	Yes	11
FASLG	NM_000639	TRCN0000059000	shL3	No	Yes	Yes	No	Yes	Yes	Yes	Yes	Yes	Yes	Yes	Yes	10
FASLG	NM_000639	TRCN0000059001	shL4	Yes	Yes	Yes	No	Yes	No	Yes	Yes	Yes	Yes	Yes	Yes	10
FASLG	NM_000639	TRCN0000058999	shL2	No	Yes	Yes	No	Yes	No	Yes	Yes	Yes	Yes	Yes	Yes	9
FASLG	NM_000639	TRCN0000059002	shL5	No	No	No	No	No	No	No	Yes	Yes	No	No	No	2
				No	**Yes**	**Yes**	**No**	**Yes**	**No**	**Yes**	**Yes**	**Yes**	**Yes**	**Yes**	**Yes**	**9**

Figure S2. Location and Effect of All si/shRNAs Targeting Either CD95L or CD95 Used in this Study and Identification of CD95 and CD95L as Critical Survival Genes in Multiple Cancer Cells using Genome-Scale Arrayed shRNA Screens, Related to Figure 1. (A) Schematic of CD95L mRNA (top) and CD95 mRNA (bottom) with the location of the 4 SmartPool siRNAs (siL1-siL4) and the shRNAs that induced DICE after transfection (siRNAs) or infection (shRNA lentiviruses) into various cancer cells. si/shRNAs that caused profound DICE (>25%) are labeled in red and ones that caused moderate DICE (10-25%) are shown in yellow. The location of the exons are shown as boxes and the location of the open reading frame is highlighted in blue. The grey line above the CD95 mRNA indicates that the 4 siRNAs of the CD95 specific SmartPools were not tested individually. **(B)** Summary of the performance of the CD95 and CD95L targeting shRNAs in the TRC library in 12 lethality screens. shRNAs scored positive (yes) when they caused cell death induction in a cell line (the mean plus 2 SD of the total cell kill induced by puromycin in untransduced cells).

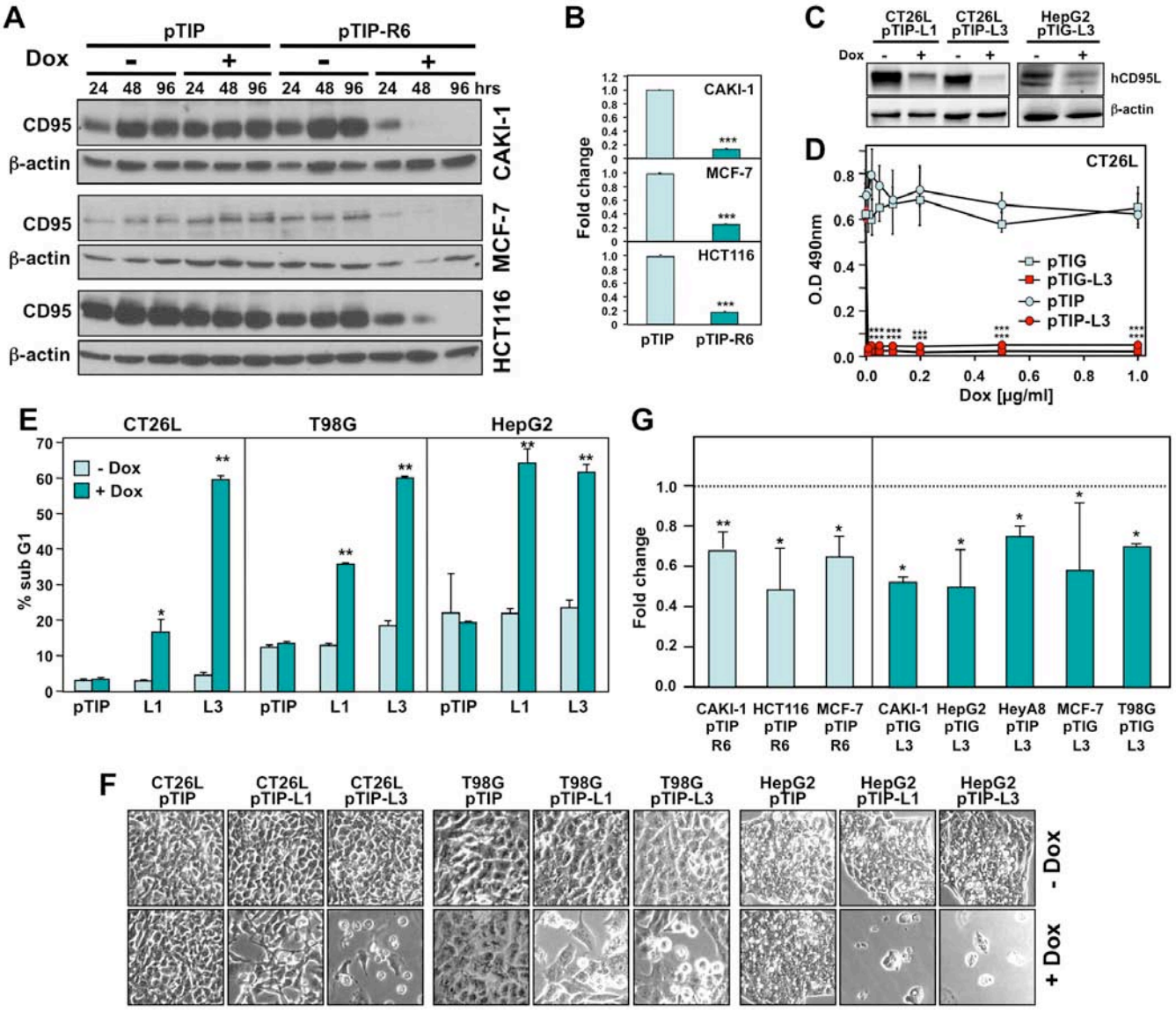

Figure S3. Characterization of Inducible CD95 and CD95L Knockdown Cells, Related to Figure 2. (A) Western blot analysis to monitor the expression of CD95 and β-actin (loading control) in CAKI-1, MCF-7, and HCT116 cells infected with either pTIP control or pTIP-R6 treated or not with Dox for the indicated times. **(B)** Quantitative real-time PCR analysis of CD95 in CAKI-1, MCF-7, and HCT116 cells infected with either pTIP control or pTIP-R6, and treated with Dox for 3 days (mean + SD of three independent cultures). P-values were calculated by t-test. *** = p<0.0001. **(C)** Western blot analysis to monitor the expression of CD95L and β-actin (loading control) in cells treated or not with Dox for 4 days (CT26L) or 1 day (HepG2). **(D)** CT26L cells were infected with pTIG, pTIG-L3, pTIP, or pTIP-L3 and treated with the indicated concentrations of Dox for 5 days; proliferation of cells was examined by SRB assay (mean + SD of three independent cultures. Two independent experiments were quantified, yielding similar results). (**E**) Quantification of cell death (nuclear PI staining) in cells infected with inducible shRNA constructs expressing two different shRNAs targeting CD95L (L1 or L3) after incubation with or without Dox for 5 days (CT26L, T98G) or 4 days (HepG2) (mean + SD of three independent cultures). P-values were calculated using *t*-test. * = p<0.01; ** = p<0.001. (**F**) Phase contrast images of the cells treated in E. Scale bar = 100 μm. **(G)** Cells stably expressing inducible CD95 or CD95L knockdown constructs were treated with Dox for 5 days, and cell survival was evaluated by MTS assay (mean + SD of three independent cultures). *p<0.05; **p<0.001. Values in graphs were normalized to control treated cells.

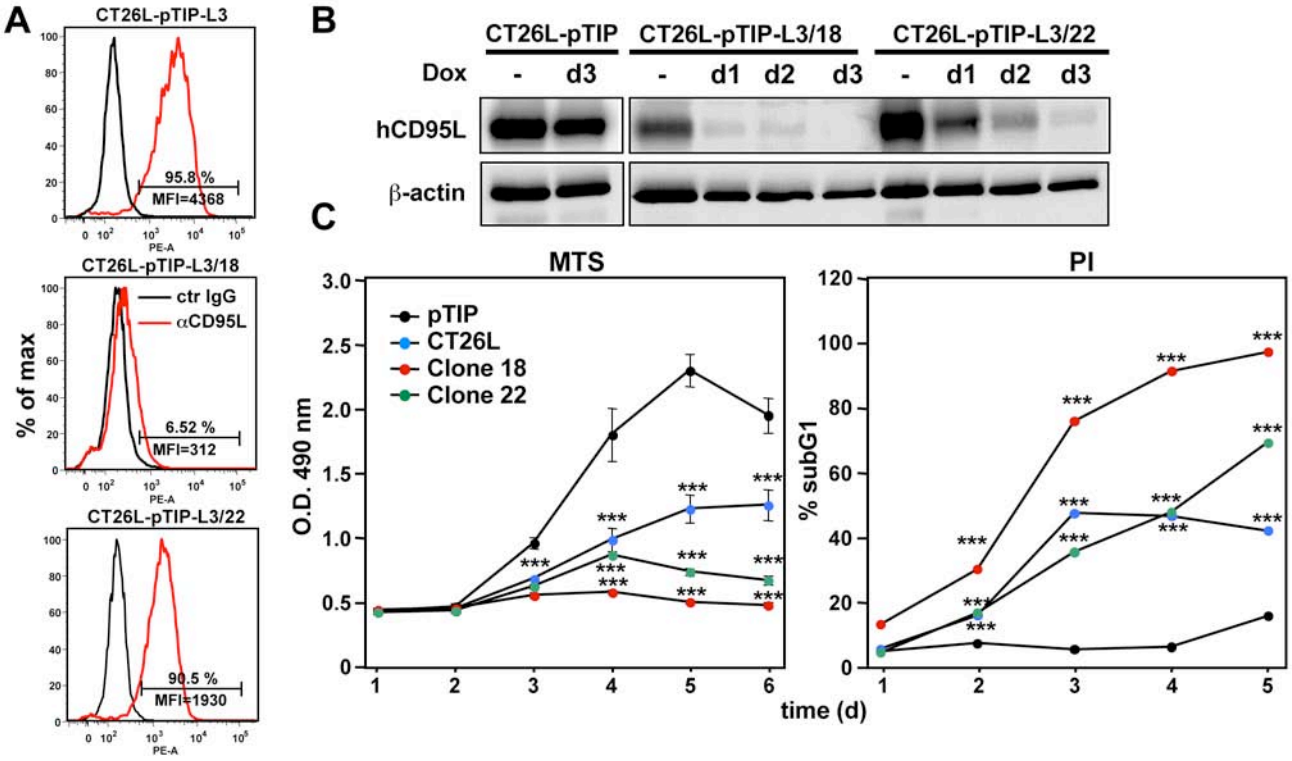

Figure S4. Characterization of Two Single Cell Clones Generated from CT26L-pTIP-L3 Cells, Related to Figure 2. **(A)** Surface staining for CD95L of parental CT26L-pTIP-L3 cells (top), clone 18 (center), and clone 22 (bottom). **(B)** Western blot analysis of human (h)CD95L and actin in control infected cells (pTIP), clone 18, and clone 22 treated or not with Dox for the indicated times. **(C)** CT26L-pTIP, CT26L-pTIP-L3/18, or CT26L-pTIP-L3/22 cells were treated with Dox for the indicated times. Cell survival was monitored by MTS assay (left panel), and DNA degradation was quantified (right panel). Values were normalized to untreated cells (mean + SD of three independent cultures). P-values were calculated using *t*-test. *** = p<0.0001.

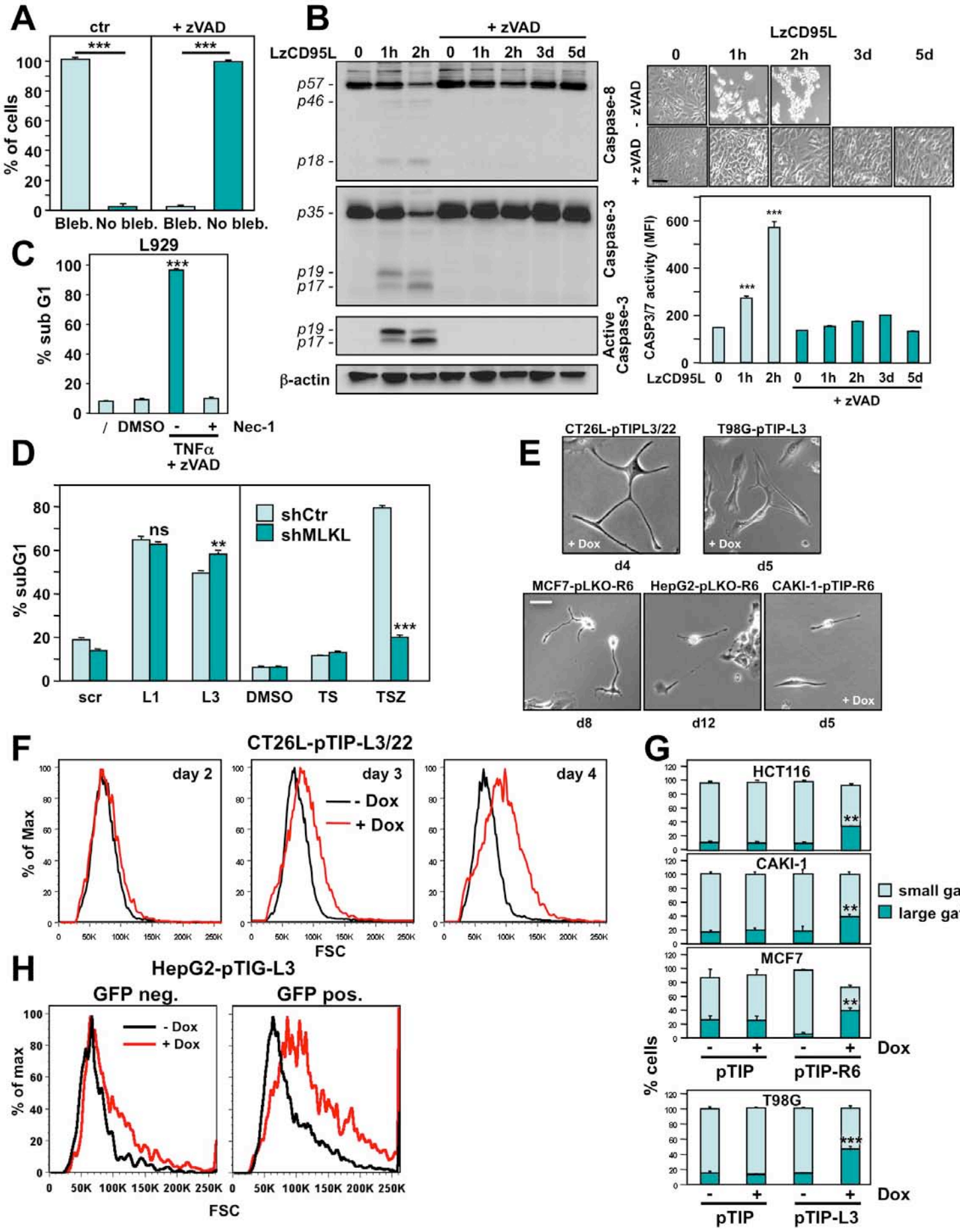
A
ctr
+ zVAD
% of cells
Bleb. No bleb. Bleb. No bleb.
B
+ zVAD
LzCD95L 0 1h 2h 0 1h 2h 3d 5d
p57 -
p46 -
p18 -
p35 -
p19 -
p17 -
p19 -
p17 -
β-actin
Caspase-8
Caspase-3
Active Caspase-3
LzCD95L
0 1h 2h 3d 5d
- zVAD
+ zVAD
CASP3/7 activity (MFI)
LzCD95L 0 1h 2h 0 1h 2h 3d 5d
+ zVAD
C
L929
% sub G1
/ DMSO - + Nec-1
TNFα
+ zVAD
D
% subG1
shCtr
shMLKL
ns
scr L1 L3 DMSO TS TSZ
E
CT26L-pTIPL3/22
T98G-pTIP-L3
+ Dox
d4
d5
MCF7-pLKO-R6
HepG2-pLKO-R6
CAKI-1-pTIP-R6
d8
d12
d5
F
CT26L-pTIP-L3/22
day 2
day 3
day 4
- Dox
+ Dox
% of Max
FSC
G
HCT116
CAKI-1
MCF7
T98G
small gate
large gate
% cells
Dox
pTIP
pTIP-R6
pTIP-L3
H
HepG2-pTIG-L3
GFP neg.
GFP pos.
- Dox
+ Dox
% of max
FSC

Figure S5. Cells Increase in Size and Lose Mitochondrial Integrity during DICE, Related to Figure 3. (**A**) CT26L-pTIP-L3/18 cells were treated with Dox with or without 20 μM zVAD-fmk for 3 days. Cells with or without blebbing were quantified using time-lapse video. At least 100 cells per sample were counted for each data point (see **Movie S2** and **S3**). P-values were calculated using *t*-test. *** = p<0.0001. **(B)** HeyA8 cells were treated with 100 ng/ml of leucine-zipper tagged (Lz)CD95L for the indicated times either with or without 20 μM of zVAD-fmk (zVAD) present. *Top left:* Western blot analysis to monitor processing of the initiator caspase 8 and the effector caspase-3. *Top right:* Phase contrast images of the treated cells. Scale bar = 100 μm. *Bottom right:* Fluorometric caspase activity assay of the treated cells (mean + SD of three independent cultures). P-values were calculated using *t*-test. *** = p<0.0001. (**C**) L929 cells were treated with 1 ng/ml TNFα and 20 μM zVAD-fmk for 18 hours after pretreatment with or without 20 μM Nec-1 (mean + SD of three independent cultures). P-value was calculated using *t*-test. *** = p<0.0001. **(D)** *Left:* Quantification of DNA fragmentation in HT-29 control infected cells and HT-29 with stable knockdown of MLKL 9 days after infection with different CD95L knockdown viruses or pLKO-scr virus. *Right*: Quantification of DNA fragmentation in cells treated for 2 days with a combination of TNFα (T, 30 ng/ml), SMAC mimetic LCL-161 (S, 50 nM), and zVAD-fmk (Z, 20 μM) (mean + SD of three independent cultures). P-values were calculated using *t*-test. ** = p<0.001; *** = p<0.0001; ns = not significant. **(E)** Phase contrast images of cell lines after either infection (pLKO-R6) or Dox treatment for the indicated times. Scale bar = 100 μm. **(F)** Representative FACS plots to determine cell size of CT26L-pTIP-L3/22 cells after treatment with Dox for the indicated time. **(G)** Cells expressing either control pTIP vector or CD95 knockdown construct were incubated with or without Dox for 4 days. Cell size was determined by gating on large and small cells in a 2D SSC/FSC FACS analysis (mean + SD of three independent cultures. Two independent experiments were quantified, yielding similar results). P-values were calculated using *t*-test. ** = p<0.001. **(H)** FACS plots to determine cell size of HepG2-pTIG-L3 cells after treatment with Dox for 3 days. GFP negative and GFP positive populations were analyzed separately.

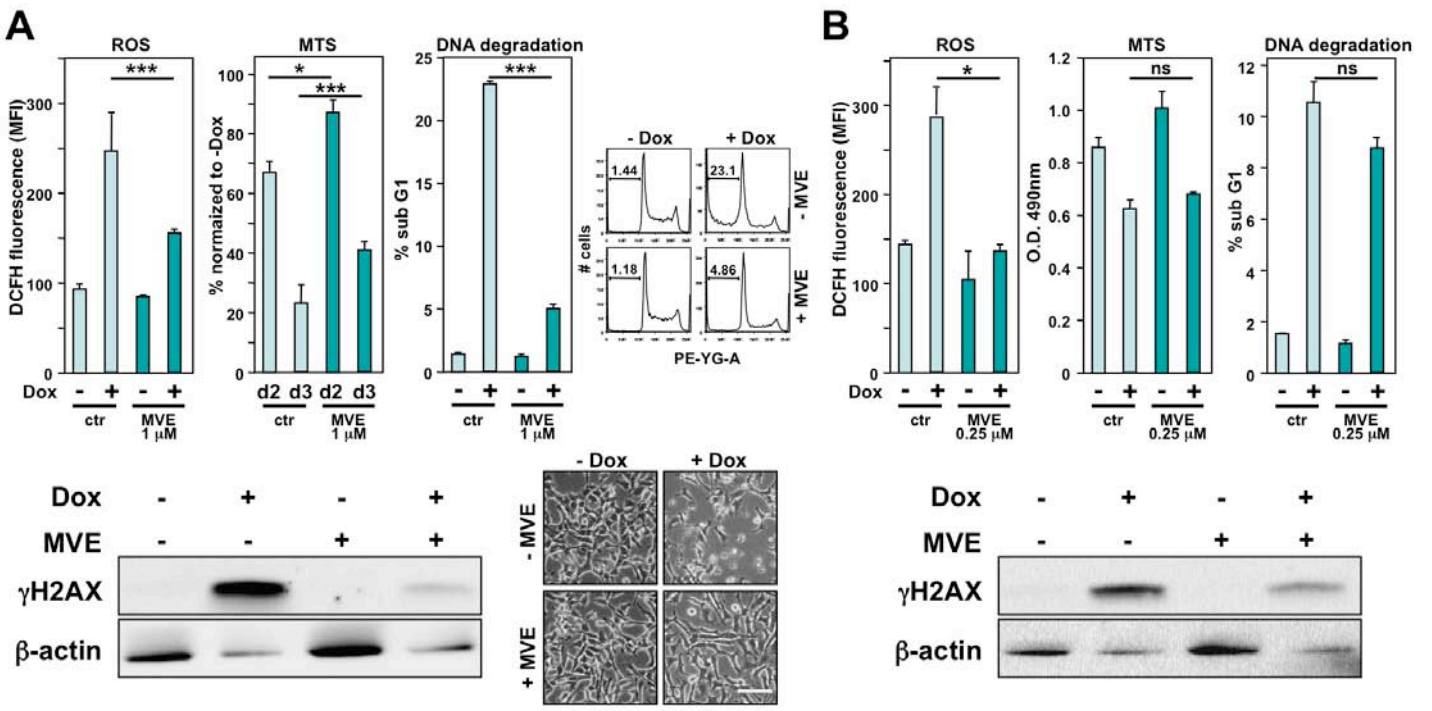

Figure S6. ROS Production during DICE Causes DNA Double Strand Breaks, Related to Figure 3. (A) *Top*, quantification of ROS production, MTS assay, and percent dead cells (PI staining) in CT26L pTIP-L3/18 cells after 2 days incubation with or without Dox and/or 1 μM MVE (ROS inhibitor). *Far right inset*, representative FACS plots of DNA degradation assay with a gate on the sub G1 fraction. P-values were calculated by ANOVA (ROS and DNA degradation) and *t*-test (MTS). * = p<0.01; *** = p<0.0001. *Bottom left*, western blot analysis of γH2AX and β-actin as loading control in cells treated for 2 days with Dox and/or MVE. *Bottom right*, representative images of the cells treated for 2 days with Dox and/or MVE. Scale bar = 100 μm. (B) *Top*, quantification of ROS production, MTS assay, and percent dead cells (PI staining) in T98G-pTIP-L3 cells after incubation with or without Dox and/or 0.25 μM MVE. Cells were treated for 4 days (ROS and MTS assay) or 3 days (DNA degradation). P-values were calculated by ANOVA. ns = non significant; * = p<0.01. *Bottom*, Western blot of γH2AX and β-actin in cells treated for 4 days with Dox and/or MVE (mean + SD of three independent cultures. Two independent experiments were quantified, yielding similar results).

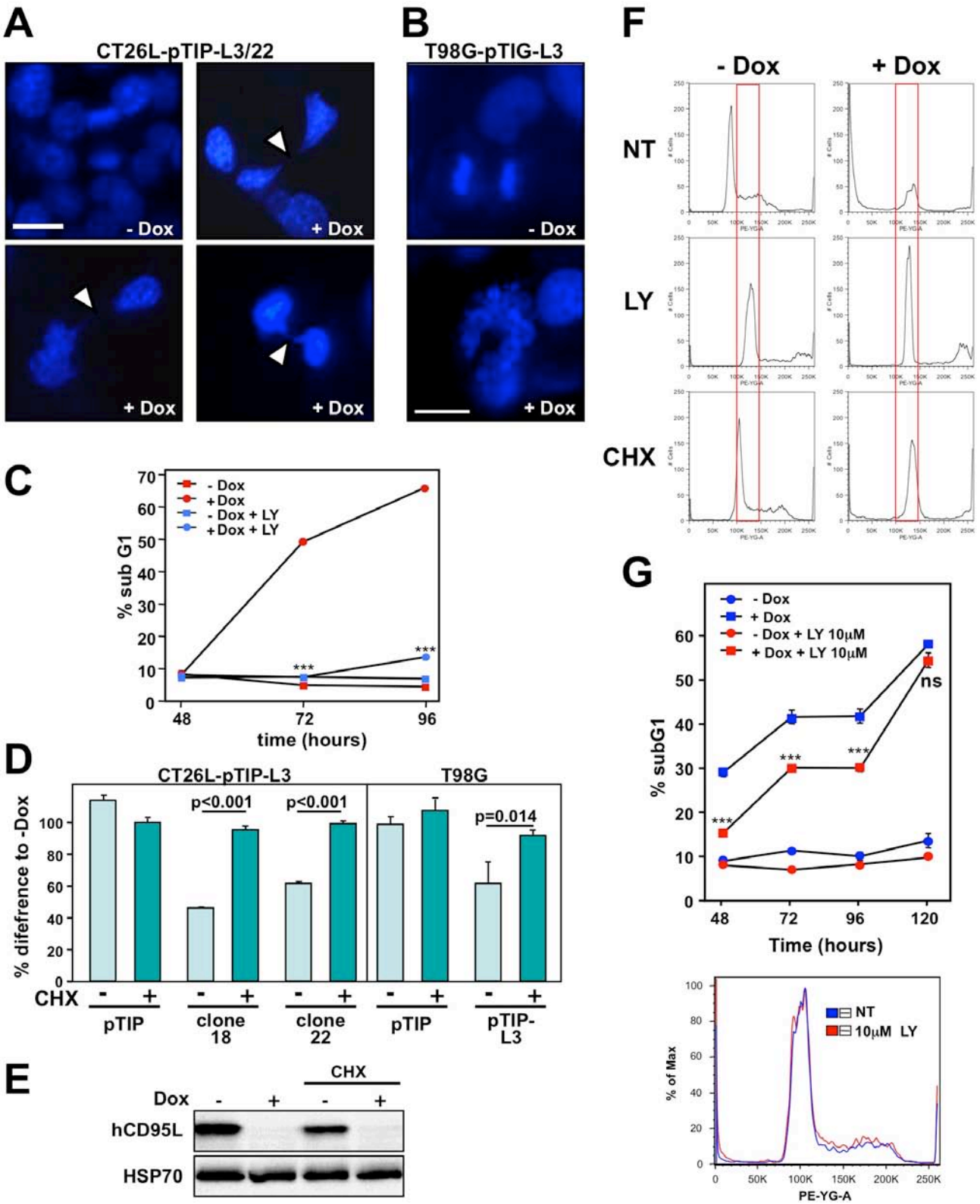

Figure S7. Anaphase Bridges in Cells Undergoing DICE and Attenuation of DICE by Arresting Cells in the Cell Cycle, Related to Figure 4. (A, B) CT26L-pTIP-L3/22 (A) and T98G-pTIG-L3 cells (B) were treated with Dox for 3 and 4 days, respectively. DNA was visualized by DAPI staining. Arrow heads indicate anaphase bridges. Size bars = 100 μm. **(C)** DNA fragmentation quantified at the indicated times points in CT26L-pTIP-L3/22 cells incubated with Dox or with media in the absence or presence of 50 μM of LY294002 (LY), the highest nontoxic dose of LY for these cells (mean + SD of three independent cultures). P-values were calculated by ANOVA. *** = p<0.0001. **(D)** CT26L-pTIP-L3 and T98G-pTIP-L3 cells were treated with Dox with or

without 0.25 μM cycloheximide (CHX) for 3 and 5 days, respectively. Cell survival was evaluated by MTS. Data are normalized to untreated cells (mean + SD of three independent cultures). P-values were calculated by *t*-test. **(E)** Western blot analysis of human (h)CD95L and HSP70 (as loading control) in CT26L-pTIP-L3/18 cells treated with Dox for 48 hours. Cells were either left untreated or were pretreated for one hour with CHX. **(F)** Cell cycle analysis using PI staining in CT26L-pTIP-L3/22 cells treated with media (NT), 50 μM LY, or 0.25 μM CHX in the presence or absence of Dox for 72 hours. The area of cells in S-phase is boxed for orientation. **(G)** *Top:* DNA fragmentation quantified at the indicated time points in T98G-pTIP-L3 cells incubated with Dox or with media in the absence or presence of 10 μM of LY294002 (LY), the highest nontoxic dose of LY for these cells (mean + SD of three independent cultures. Two independent experiments were quantified, yielding similar results). P-values were calculated by ANOVA. *** = $p<0.0001$; ns = not significant. *Bottom:* FACS profile of T98G-pTIP-L3 cells after nuclear PI staining treated with media (NT) or 10 μM LY in the presence or absence of Dox for 72 hours.

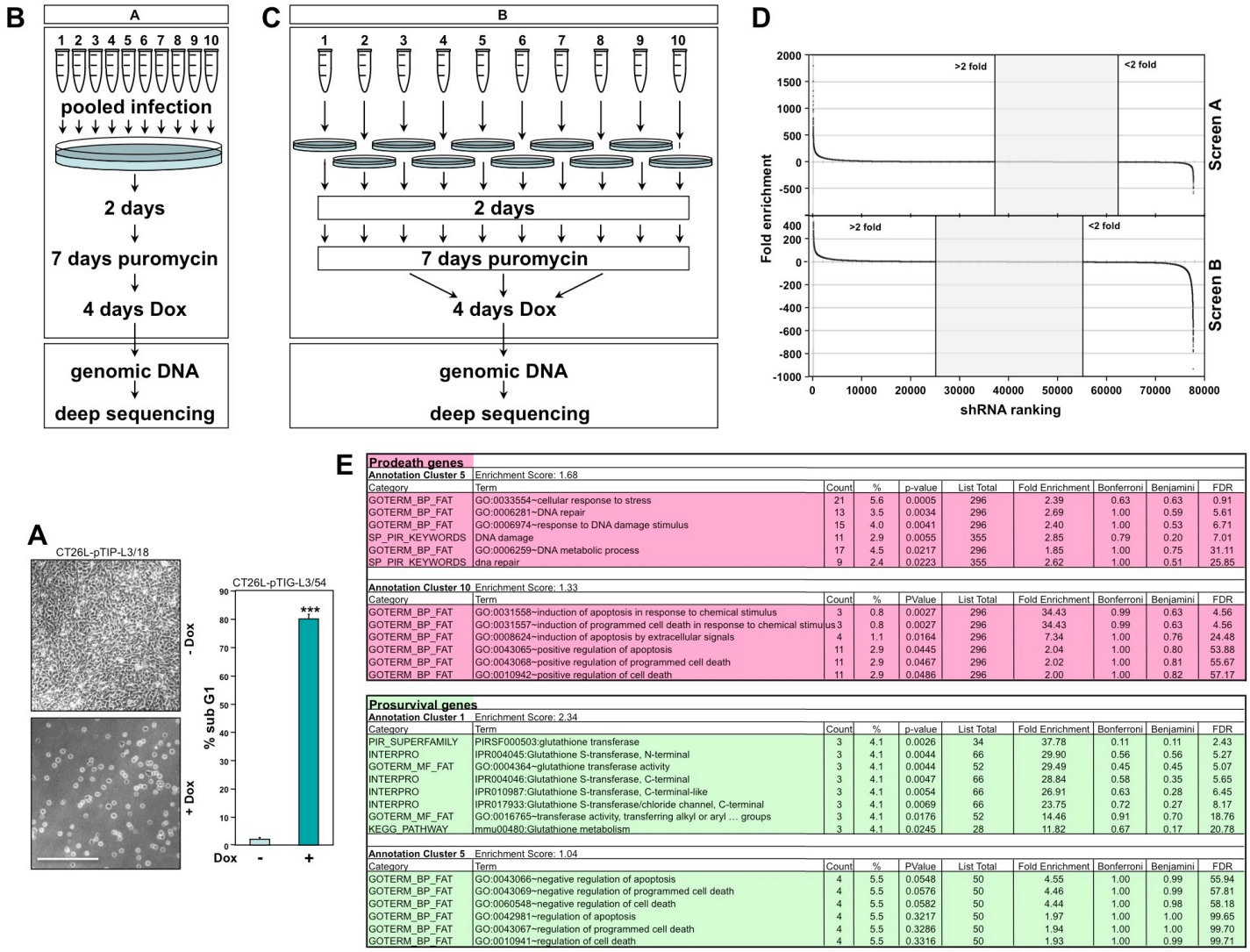

E

Prodeath genes

Annotation Cluster 5	Enrichment Score: 1.68								
Category	Term	Count	%	p-value	List Total	Fold Enrichment	Bonferroni	Benjamini	FDR
GOTERM_BP_FAT	GO:0033554~cellular response to stress	21	5.6	0.0005	296	2.39	0.63	0.63	0.91
GOTERM_BP_FAT	GO:0006281~DNA repair	13	3.5	0.0034	296	2.69	1.00	0.59	5.61
GOTERM_BP_FAT	GO:0006974~response to DNA damage stimulus	15	4.0	0.0041	296	2.40	1.00	0.53	6.71
SP_PIR_KEYWORDS	DNA damage	11	2.9	0.0055	355	2.85	0.79	0.20	7.01
GOTERM_BP_FAT	GO:0006259~DNA metabolic process	17	4.5	0.0217	296	1.85	1.00	0.75	31.11
SP_PIR_KEYWORDS	dna repair	9	2.4	0.0223	355	2.62	1.00	0.51	25.85

Annotation Cluster 10	Enrichment Score: 1.33								
Category	Term	Count	%	PValue	List Total	Fold Enrichment	Bonferroni	Benjamini	FDR
GOTERM_BP_FAT	GO:0031558~induction of apoptosis in response to chemical stimulus	3	0.8	0.0027	296	34.43	0.99	0.63	4.56
GOTERM_BP_FAT	GO:0031557~induction of programmed cell death in response to chemical stimulus	3	0.8	0.0027	296	34.43	0.99	0.63	4.56
GOTERM_BP_FAT	GO:0008624~induction of apoptosis by extracellular signals	4	1.1	0.0164	296	7.34	1.00	0.76	24.48
GOTERM_BP_FAT	GO:0043065~positive regulation of apoptosis	11	2.9	0.0445	296	2.04	1.00	0.80	53.88
GOTERM_BP_FAT	GO:0043068~positive regulation of programmed cell death	11	2.9	0.0467	296	2.02	1.00	0.81	55.67
GOTERM_BP_FAT	GO:0010942~positive regulation of cell death	11	2.9	0.0486	296	2.00	1.00	0.82	57.17

Prosurvival genes

Annotation Cluster 1	Enrichment Score: 2.34								
Category	Term	Count	%	p-value	List Total	Fold Enrichment	Bonferroni	Benjamini	FDR
PIR_SUPERFAMILY	PIRSF000503:glutathione transferase	3	4.1	0.0026	34	37.78	0.11	0.11	2.43
INTERPRO	IPR004045:Glutathione S-transferase, N-terminal	3	4.1	0.0044	66	29.90	0.56	0.56	5.27
GOTERM_MF_FAT	GO:0004364~glutathione transferase activity	3	4.1	0.0044	52	29.49	0.45	0.45	5.07
INTERPRO	IPR004046:Glutathione S-transferase, C-terminal	3	4.1	0.0047	66	28.84	0.58	0.35	5.65
INTERPRO	IPR010987:Glutathione S-transferase, C-terminal-like	3	4.1	0.0054	66	26.91	0.63	0.28	6.45
INTERPRO	IPR017933:Glutathione S-transferase/chloride channel, C-terminal	3	4.1	0.0069	66	23.75	0.72	0.27	8.17
GOTERM_MF_FAT	GO:0016765~transferase activity, transferring alkyl or aryl … groups	3	4.1	0.0176	52	14.46	0.91	0.70	18.76
KEGG_PATHWAY	mmu00480:Glutathione metabolism	3	4.1	0.0245	28	11.82	0.67	0.17	20.78

Annotation Cluster 5	Enrichment Score: 1.04								
Category	Term	Count	%	PValue	List Total	Fold Enrichment	Bonferroni	Benjamini	FDR
GOTERM_BP_FAT	GO:0043066~negative regulation of apoptosis	4	5.5	0.0548	50	4.55	1.00	0.99	55.94
GOTERM_BP_FAT	GO:0043069~negative regulation of programmed cell death	4	5.5	0.0576	50	4.46	1.00	0.99	57.81
GOTERM_BP_FAT	GO:0060548~negative regulation of cell death	4	5.5	0.0582	50	4.44	1.00	0.98	58.18
GOTERM_BP_FAT	GO:0042981~regulation of apoptosis	4	5.5	0.3217	50	1.97	1.00	1.00	99.65
GOTERM_BP_FAT	GO:0043067~regulation of programmed cell death	4	5.5	0.3286	50	1.94	1.00	1.00	99.70
GOTERM_BP_FAT	GO:0010941~regulation of cell death	4	5.5	0.3316	50	1.93	1.00	0.99	99.71

Figure S8. Genome-Wide shRNA Screen to Identify Genes that Modulate DICE, Related to Table S4. (A) *Left:* Phase contrast images of CT26L-pTIP-L3/18 cells treated or not with Dox for 4 days. Scale bar = 100 μm. *Right:* Quantification of DNA degradation in CT26L-pTIG-L3/54 cells treated or not with Doxycycline for 2 days (mean + SD of three independent cultures. Two independent experiments were quantified, yielding similar results). P-values were calculated using *t*-test ** = p<0.001; *** = p<0.0001. **(B, C)** Flow charts illustrating the design of the two shRNA screens using the shRNAs provided in 10 different pools (see text for details). **(D)** All 77,720 shRNAs in screen A (top) and B (bottom) identified by deep sequencing ranked according to fold enrichment of isolated PCR fragments containing the integrated shRNAs. Grey areas in the center contain fragments that were not enriched or underrepresented in cells after addition of Dox (cutoff = 2-fold). **(E)** DAVID gene ontology analysis of overrepresented (prodeath) or underrepresented (prosurvival) genes. Selected highly enriched clusters are shown. For a list of genes, see **Table S4**.

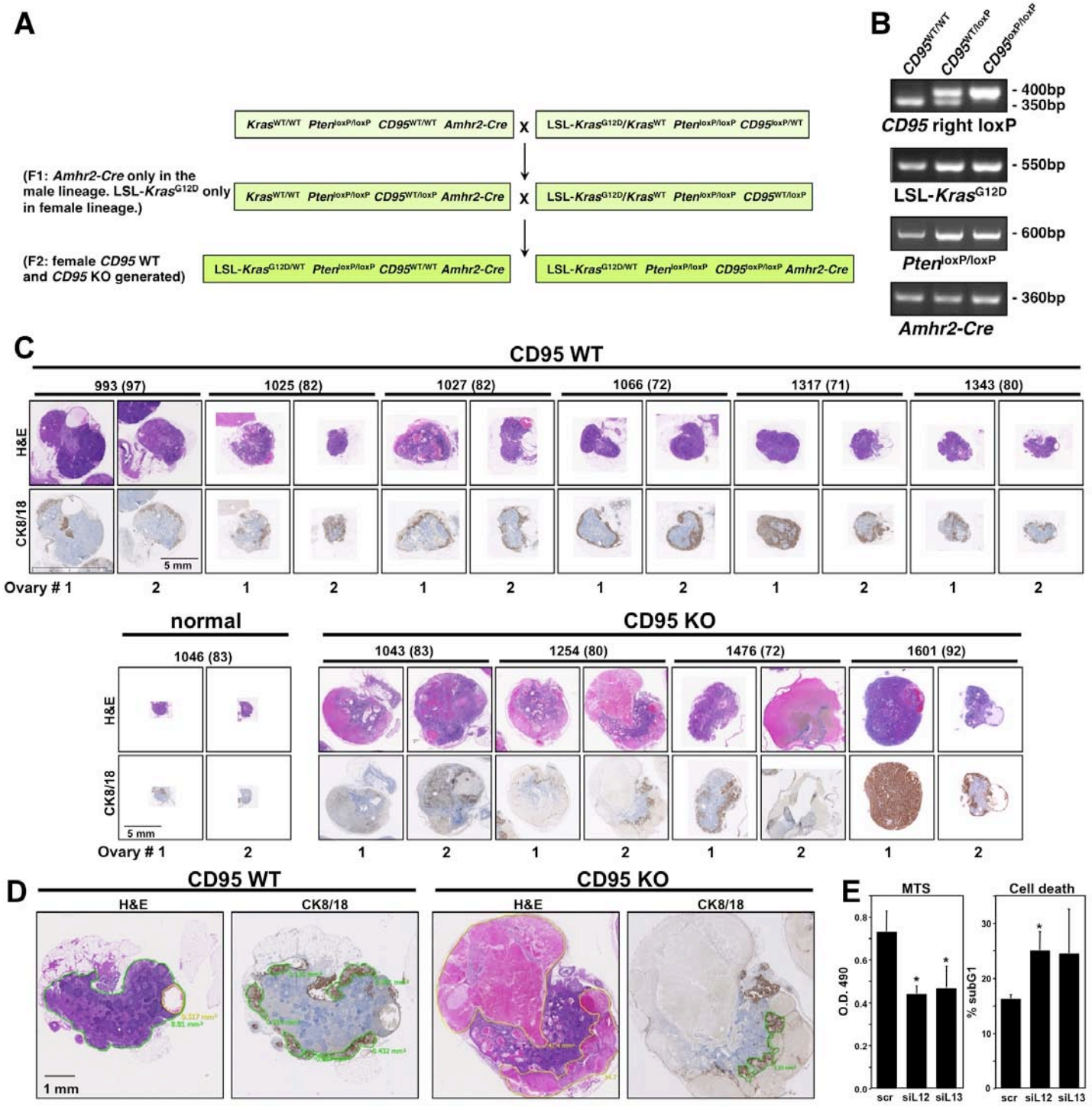

Figure S9. Generation of LSL-*Kras*$^{G12D/WT}$*Pten*$^{loxP/loxP}$*CD95*$^{loxP/loxP}$*Amhr2-Cre* Mice and Analysis of their Ovaries, Related to Figure 6. (A) Breeding scheme to generate female "CD95-WT-mice" with the genotype LSL-*Kras*$^{G12D/WT}$*Pten*$^{loxP/loxP}$*CD95*$^{WT/WT}$*Amhr2-Cre* and "CD95-KO-mice" with the genotype LSL-*Kras*$^{G12D/WT}$*Pten*$^{loxP/loxP}$*CD95*$^{loxP/loxP}$*Amhr2-Cre*. **(B)** Representative PCR analyses to document the generation of the *CD95* knockout mice. *CD95* WT, heterozygous, and homozygous *CD95* knockout mice showed a band for LSL-*Kras*^{G12D}, *Pten*$^{loxP/loxP}$ and *Amhr2-Cre* (bottom three panels). The genotype differed in the presence of the loxP site in the *CD95* gene. Shown is the PCR analysis of the right loxP site in three genotypes differing in the presence of *CD95* loxP sites (top panel). **(C)** H&E staining and immunohistochemistry for cytokeratin 8/18 of 6

CD95 wild-type mice and 4 *CD95* knockout mice. Shown are both ovaries for each mouse at the same magnification. Shown are mouse ear tag numbers and the age of each mouse at sacrifice (in brackets). **(D)** Example of the morphometric analysis used to quantify areas of tumor and necrosis/hemorrhage in two representative ovaries. **(E)** Effect of two mouse CD95L targeting shRNAs on growth and viability of P1 cells after sequential transfection with two mouse CD95L specific siRNAs (mean + SD of three independent cultures). P-values were calculated using *t*-test. * = $p<0.05$.

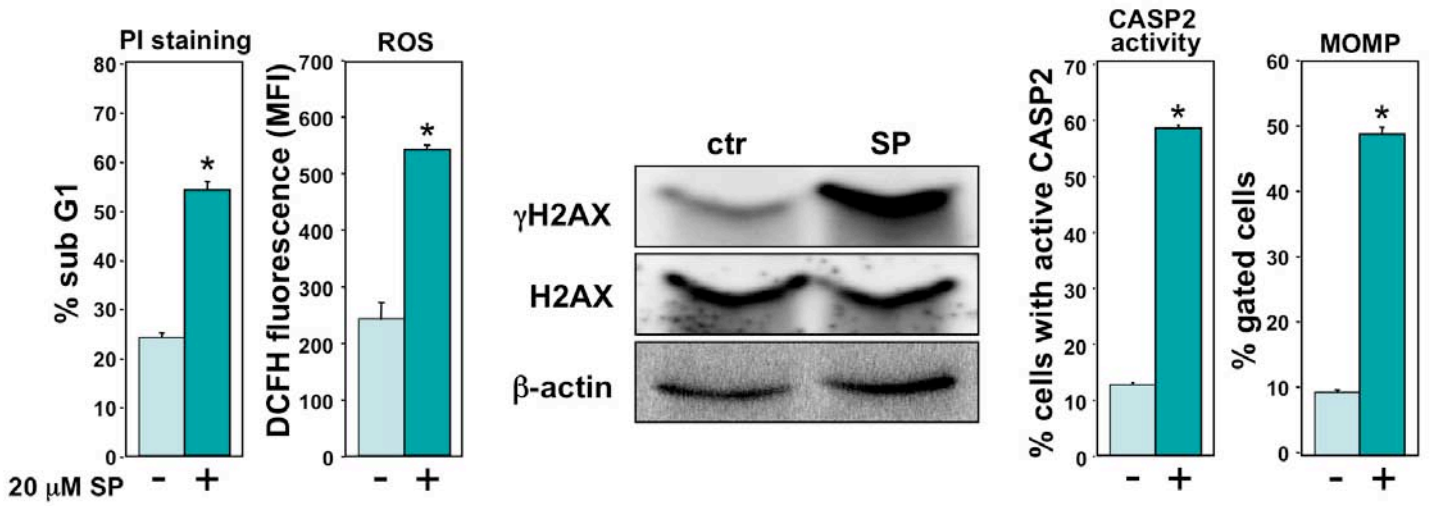

Figure S10: Inhibition of JNK Causes Features of DICE in T98G Cells, Related to Supplementary Discussion. T98G cells treated with 20 μM of SP600125 for 4 days. Quantification of DNA degradation, ROS production, caspase-2 activity, MOMP, and Western blot for γH2AX and H2AX are shown (mean + SD of three independent cultures). P-values were calculated using *t*-test. * = p<0.01.

Table S1: Cell Lines in which DICE Was Observed, Related to Figure 1.

Cell line	Cancer type	p53 status	siCD95L pool or siRNAs	pLKO-R6	pLKO-R2	pLKO-L1	pLKO-L2	pLKO-L3	pLKO-L4	pTIP-R6	pTIG-L3	pTIP-L3	pTIP-L1
SKOV3ip1	Ovarian	mut[1]	nd	O[1]	nd	X	nd	X	X	O[2]	nd	nd	nd
HeyA8	Ovarian	wt[2]	X	X	nd	X	nd	X	X	O[2]	O	nd	nd
HepG2	Liver	wt[3]	O[1]	O[1]	nd	X	O[1]	X	X	nd	X	X	X
MCF7	Breast	wt[1]	X	X	X	X	nd	X	X	X	O	nd	nd
MCF10A	Breast	wt[4]	nd	nd	nd	nd	nd	nd	nd	nd	O	nd	nd
MDA-MB-231	Breast	mut[1]	nd	nd	nd	nd	nd	X	nd	nd	nd	X	nd
HeLa	Cervical	wt[5]	nd	X	nd	nd	nd	X	nd	nd	nd	nd	nd
HCT116	Colon	wt[1]	nd	X	nd	X	nd	X	X	X	nd	X	nd
HCT116 p53-/-	Colon	ko[6]	nd	nd	nd	nd	nd	nd	nd	X	nd	X	nd
HT-29	Colon	mut[5]	nd	nd	nd	X	nd	X	nd	nd	nd	nd	nd
CAKI-1	Renal	wt[1]	nd	O[1]	nd	X	nd	X	X	O	nd	nd	nd
T98G	GBM	mut[7]	nd	X	nd	X	nd	X	X	nd	X	X	X
U87MG	GBM	wt[8]	nd	nd	nd	nd	nd	nd	nd	O	O	nd	nd
NB7	Neuroblastoma	mut[9]	nd	nd	nd	nd	nd	nd	nd	X	nd	X	nd
CT26L	Colon (mouse)	wt[10]	nd	na	na	X	nd	X	X	na	X	X	X
PKOSE-1	Ovarian (mouse)	wt[11]	X	na	na	na	na	na	na	na	na	na	na

(1) (O'Connor et al., 1997); (2) (Modesitt et al., 2001), (3) (Vollmer et al., 1999); (4) (Bianco et al., 1994); (5) http://p53.free.fr/Database/Cancer_cell_lines/p53_cell_lines.html; (6) (Bunz et al., 1998); (7) (Van Meir et al., 1994); (8) (Wischhusen et al., 2003); (9) http://cancer.sanger.ac.uk/cosmic/sample/overview?id=949174; (10) (Luo et al., 2004); (11) (Mullany et al., 2011).

- **O** Reduction in growth
- **X** Growth reduction and death
- na Not applicable
- nd Not done
- 1 Previous results (Chen et al., 2010)
- 2 Death through leakiness of Tet inductible vector

Table S2: Examples of Critical Survival Genes Identified in 12 Genome-Wide shRNA Lethality Screens, Related to Figure 1.

Gene	RefSeq	# of Cell Lines Affected	Ontologies	Description
Cell cycle and mitosis				
AURKA	NM_003600	9	GO:0000278	*Mitotic cell cycle*
CDK4	NM_000075	10	GO:0000278	*Mitotic cell cycle*
CDK6	NM_001259	10	GO:0000278	*Mitotic cell cycle*
CHEK1	NM_001274	10	GO:0000278	*Mitotic cell cycle*
INCENP	NM_020238	9	GO:0000278	*Mitotic cell cycle*
PLK1	NM_005030	12	GO:0000278	*Mitotic cell cycle*
TUBB3	NM_006086	10	GO:0000278	*Mitotic cell cycle*
RAN	NM_006325	9	GO:0000278	*Mitotic cell cycle*
Cell growth				
EIF3B	NM_003751	9	GO:0006414	*Translation elongation*
EIF3F	NM_003754	9	GO:0006414	*Translation elongation*
EIF3H	NM_003756	9	GO:0006414	*Translation elongation*
EIF3S8	NM_003752	9	GO:0006414	*Translation elongation*
EIF4A3	NM_014740	10	GO:0006414	*Translation elongation*
EIF4EBP1	NM_004095	10	GO:0006414	*Translation elongation*
RPL10A	NM_007104	11	GO:0006414	*Translation elongation*
RPL11	NM_000975	9	GO:0006414	*Translation elongation*
RPL14	NM_003973	9	GO:0006414	*Translation elongation*
RPL18	NM_000979	10	GO:0006414	*Translation elongation*
RPL3	NM_000967	9	GO:0006414	*Translation elongation*
RPL31	NM_000993	10	GO:0006414	*Translation elongation*
RPL4	NM_000968	9	GO:0006414	*Translation elongation*
RPL6	NM_000970	10	GO:0006414	*Translation elongation*
RPL9	NM_000661	10	GO:0006414	*Translation elongation*
RPS11	NM_001015	9	GO:0006414	*Translation elongation*
RPS17	NM_001021	9	GO:0006414	*Translation elongation*
RPS18	NM_022551	11	GO:0006414	*Translation elongation*
RPS28	NM_001031	9	GO:0006414	*Translation elongation*
RPS3	NM_001005	11	GO:0006414	*Translation elongation*
RPS4X	NM_001007	9	GO:0006414	*Translation elongation*
RPS5	NM_001009	9	GO:0006414	*Translation elongation*
RPS6	NM_001010	9	GO:0006414	*Translation elongation*
Oncogenes				
HDAC1	NM_004964	9	GO:0042981	*Regulation of apoptosis*
HRAS	NM_176795	9	GO:0012501	*Programmed cell death*
KRAS	NM_033360	10	GO:0012501	*Programmed cell death*
NRAS	NM_002524	9	GO:0012501	*Programmed cell death*
Cell death				
FASLG	**NM_000639**	**9**	**GO:0012501**	***Programmed cell death***
MCL1	NM_021960	10	GO:0012501	*Programmed cell death*
RIPK1	NM_003804	9	GO:0012501	*Programmed cell death*
Cytoskeleton				
TUBA1C	NM_032704	12	GO:0015630	*Microtubule cytoskeleton*

Table S3: List of Compounds Tested for their Activity to Modulate DICE, Related to Figure 5.

Pathway inhibitors (tested on CT26L-pTIP-L3/18 cells -/+ Dox by quantifying % sub G1 cells 48 hours after addition of Dox).

Inhibitor*	**Target**	**Source**	**Concentration**
Olaparib (AZD2281, KU0059436)	PARP	Selleckchem	1 μM
NU7441 (KU57788)	DNAPK	Selleckchem	10 μM
KU60019	ATM	Selleckchem	10 μM
3-Aminobenzamide (3-AB)	PARP	Sigma	5 μM
Cyclosporin A	Mitochondrial transition pore	Sigma	0.5 μM
CHIR124	Chk1	Selleckchem	0.05 μM
GO6976	PKC	Sigma	0.5 μM
Bay 11.7082	NF-kB	Sigma	0.5 μM
MK2206	AKT	Selleckchem	1 μM
Camptothecin	DNA Topoisomerase	Sigma	0.05 μM
CKI7	Casein Kinase 1	Sigma	20 μM
7Bio	Aurora kinase	Millipore	2 μM
zVDVAD	Caspase-2	Enzo	20 μM
zVAD	Pan caspase inhibitors	Enzo	20 μM
Cycloheximide (CHX)	Translation inhibitor	Sigma	0.25 μM
Necrostatin	RIP1	Sigma	20 μM

* cells were preincubated for 1 hour with each compound before addition of Dox.

Chemotherapeutic drugs (tested on both CAKI-1-pTIP-R6 and HCT116-pTIP-R6 cells by performing MTS assays 1, 4, and 5 days after addition of Dox).

Drug	**Source**	**Concentration**
Taxol	Sigma	10 nM
Etoposide	Sigma	1 μM
Doxorubicine	Sigma	100 ng/ml
Carboplatin	Sigma	100 ng/ml

For each of the compounds, toxicity was determined by titering the compounds onto the cells and then selecting the highest nontoxic concentration.

Table S4: Results of Genome-Wide shRNA Screen Combined with Deep Sequencing (Excel file), **Related to Figure 5.**

Table S5: Primers Used for Genotyping, Related to Supplementary Methods.

Gene name	Predicted PCR products	Primer 1 sequence	Primer 2 sequence
LSL-Kras G12D	$Kras^{WT}$: none; LSL-$Kras^{G12D}$: 550 bp	AGCCACCATGGCTTGAGTAA	CTTTACAAGCGCACGCAGAC
Pten deletion	$Pten^{Del}$: 300 bp.	ACTCAAGGCAGGGATGAGC	GCTTGATATCGAATTCCTGCAGC
Pten (left loxP site)	$Pten^{WT/WT}$: 1000 bp; $Pten^{WT/loxP}$: 1000+1200 bp; $Pten^{loxP/loxP}$: 1200 bp.	ACTCAAGGCAGGGATGAGC	AATCTAGGGCCTCTTGTGCC
CD95 (right loxP site)	$CD95^{WT/WT}$: 350 bp; $CD95^{WT/loxP}$: 350+400 bp; $CD95^{loxP/loxP}$: 400 bp	GCTGTGTCTATCAGTCTC	AAGAGACCCACCTCTAGGTAG
CD95 deletion	$CD95^{WT}$: none; $CD95^{loxP}$: none; $CD95^{Del}$: 350 bp.	CTGTGGTGGGAGAACTGGAT	TGGGTATGCTCCAGATAGGC
CD95 Exon 9	$CD95^{WT}$: 338 bp; $CD95^{loxP}$: 338 bp; $CD95^{Del}$: none.	ATGCATGACAGCATCCAAGA	TGCTGGCAAAGAGAACACAC
Amhr2-Cre	Cre+: 360 bp; Cre-: none	CGCATTGTCTGAGTAGGTGT	GAAACGCAGCTCGGCCAGC

Supplementary Movies:

Movie S1: Time-Lapse Video Analysis of CT26L-pTIP-L3/18 Cells after Addition of Dox, Related to Figure S4.

Movie S2: Time-Lapse Video Analysis of CT26L-pTIP-L3/18 Cells after Addition of Dox Pretreated with DMSO Control, Related to Figure 3.

Movie S3: Time-Lapse Video Analysis of CT26L-pTIP-L3/18 Cells after Addition of Dox Pretreated with zVAD-fmk Control, Related to Figure 3.

Movie S4: Time-Lapse Video Analysis of a CT26L-pTIP-L3/18 Cell after Addition of Dox, Related to Figure 4. Arrow head labels a single cell that attempts to divide and ends up with a fragmented nucleus.

Movie S5: Time-Lapse Video Analysis of a CT26L-pTIP-L3/18 Cell after Addition of Dox, Related to Figure 4. Arrow head labels a single cell that completes cytokinesis, but both daughter cells die shortly after cell division.

Movie S6: Time-Lapse Video Analysis of T98G-pTIG-L3 Cells after Addition of Dox, Related to Figure 4. Note that many cells round up and die after they enter mitosis as seen by the appearance of metaphase plates in these cells.

SUPPLEMENTARY RESULTS

DICE Engages a Complex Cell Death Program that Is Difficult to Block

Autophagy is turned on in CT26L cells undergoing DICE (data not shown). However, since neither the knockdown of ATG5 nor the treatment with the autophagy inhibitor 3-MA significantly altered the kinetics of DICE, we concluded that at least in CT26L cells, autophagy, while being a sign of stress, did not contribute to or prevent DICE execution (**Figure 5L**, and data not shown).

We found two compounds that delayed DICE for about a week before cells died: the PI3K inhibitor LY294002 (LY) and the protein translation inhibitor cycloheximide (CHX). Treatment with 50 μM LY severely slowed down DICE (**Figure S7C**). When treated with low concentrations of CHX (0.25 μM), neither CT26L-pTIP-L3 clone 18, clone 22, nor T98G cells died from CD95L knockdown within the time frame of the experiment (**Figure S7D**). The expression of the shRNA was not affected, and CD95L was efficiently knocked down in CHX treated cells (**Figure S7E**). Because all drugs that delayed DICE were ones that prevented cells to traverse through the cell cycle, we tested whether CHX and LY affected cell cycle progression. Consistent with their reported activity as cell cycle inhibitors (Casagrande et al., 1998; Liu et al., 2010), treatment of CT26L-pTIP-L3/18 cells with either compound induced a G1 cell cycle arrest, and it appeared that after addition of Dox, cells accumulated at the G2/M point of the cell cycle (**Figure S7F**), providing an explanation for why they did not die immediately. Interestingly, LY did not induce a cell cycle arrest in T98G cells and consequently did not block DICE induction in these cells (**Figure S7G**), supporting the conclusion that multiple compounds with very different targets in the cells can slow down DICE when causing cell cycle arrest.

In order to identify genes that could modulate DICE, we combined a genome-wide shRNA screen with next generation sequencing. By isolating genomic DNA and quantifying all shRNAs that had integrated into the genome by deep sequencing, we identified underrepresented shRNAs (DICE attenuators) and enriched shRNAs (DICE promoters) by ranking all shRNAs according to the number of detected reads. These numbers were compared to cells that had only been infected with the shRNA library without knockdown of CD95L. The screen was performed twice (screen A and screen B, see method section for details) (**Figure S8B** and **C**). Between 2 and 4 million reads per sample with unique alignments were obtained, and all samples were ranked from highest overrepresentation to highest underrepresentation (**Figure S8D**). Only genes were considered that were targeted by two or more shRNAs (**Table S4**). In total, in both screens, combined reads of 10 or more (in both the minus plus Dox conditions) were detected for 59,907 of the shRNAs, representing a 77% coverage of the genome by the shRNA library.

JNK May Be Part of a Set of Pathways that Protect Cancer Cells from DICE

We previously reported a correlation between the activation of JNK kinases and the tumorigenic activity of CD95 (Chen et al., 2010). We therefore wondered whether inhibition of JNK would induce cell death and whether this would have some of the features seen in cells undergoing DICE. T98G cells were treated for 4 days with 20 μM of the JNK inhibitor SP600125 (**Figure S10**). This treatment induced cell death, generated ROS, caused DSBs as evidenced by an increase in γH2AX, resulted in activation of caspase-2, and caused MOMP showing similarities to DICE.

SUPPLEMENTARY DISCUSSION

Most cancer cells were more effectively killed by knockdown of CD95L than by knockdown of CD95. We hypothesize that the reason for this is that the ligand is often less abundant than the receptor and is more likely to become limiting. We went to great lengths to establish that the cell death we describe is caused by the elimination of either CD95 or CD95L. We have used a total of 15 CD95/CD95L specific si/shRNAs to induce DICE in various cancer cells, and the effects of siRNAs were dose dependent. A mutated siRNA that failed to knockdown CD95L did not induce DICE. Interestingly, however, we failed to prevent DICE by reconstituting cells with a siRNA resistant version of CD95L. We found that introduction of silent mutations into the site of the CD95L mRNA targeted by shL3 altered the expression, localization, migration behavior on SDS-PAGE,

and stability of the CD95L protein in a way that it may not have the same activity anymore, an effect that has been reported for MDR-1 before (Kimchi-Sarfaty et al., 2007).

DICE may also occur *in vivo*. In the ovarian cancer model used, cancer developed after activation of oncogenic *Kras* and deletion of *Pten* in the ovaries. In three of the four *CD95* knockout mice studied, most of the ovarian tissue was replaced by necrotic tissue with signs of massive hemorrhage at around 80 days. This was not seen in any of the six cancerous mice expressing wild-type *CD95*. In one of the *CD95* knockout mice, we detected evidence of ongoing necrosis. However, since dead cells are eliminated quickly *in vivo*, detecting ongoing cell death in a tumor model is often challenging. Interestingly, when mice were analyzed earlier at day 43, early dysplastic tissue formed in both wild-type and *CD95* mutant tumors, and all cancer cells expressed CD95 (data not shown), suggesting that the selection for cancer cells that retain CD95 starts early at neoplastic transformation in this model. To exclude the possibility that Cre could not recombine CD95 at all, we infected the clone that had retained both floxed CD95 alleles (see **Figure 7C**, lane 6) with adenoviral Cre. This resulted in complete deletion of both CD95 alleles (data not shown), supporting our conclusion that lack of CD95 deletion in tumor cells was not due to an inability to recombine, but more likely the result of a stochastic selection process against loss of CD95. This was also supported by our finding that almost all cancerous nodules in the livers of DEN treated *CD95*$^{loxP/loxP}$*Alb-Cre* mice showed expression of CD95.

We found that treatment with CD95L inhibitors has some growth inhibiting effect on a small number of cancer cells lines without inducing cell death (data not shown). We recently found that CD95L in cancer cell lines is mostly localized intracellularly and is likely not accessible to CD95L neutralizing proteins (data not shown). In contrast, targeting the CD95L mRNA was much more effective in killing cells, and efforts to target CD95L mRNA for cancer therapy are ongoing.

A Hypothesis on the Physiological Role of DICE

CD95L induced apoptosis is one of two mechanisms that cytotoxic killer cells use to eliminate virus infected or transformed cells. If it fails, then cancer can develop. We now propose that transformed cells and cells in rapidly proliferating tissues under conditions that can lead to neoplastic transformation (e.g. compensatory proliferation of liver tissue) must receive a low level signal through CD95 to survive. If CD95 or its stimulating ligand are completely removed, then cells die. According to this model, CD95 and CD95L are part of a fail-safe mechanism to prevent the occurrence of CD95 deficient cancer cells that can no longer be targeted by immune cells that secrete CD95L.

SUPPLEMENTARY METHODS

Reagents and Antibodies

Reagents were obtained from the following sources: anti-ß-actin antibody (clone #I-19) and anti-hCD95 (clone #C-20) (Santa Cruz); anti-phospho(γ)H2AX and anti-H2AX (Calbiochem); and anti-mouse CD95 sc-1024 (Santa Cruz); anti-human CD95L #556387 (BD Biosciences); and anti-HSP70 (BD Biosciences); mouse anti-β-tubulin (CHEMICON International); rat monoclonal anti-caspase-2 (11B4) and goat anti-rat IgG, HRP conjugated (Enzo Life Science); goat anti-mouse IgG, HRP-conjugated, rabbit anti-goat IgG, HRP-conjugated, and goat anti-rabbit IgG, HRP-conjugated (Southern Biotech); zVAD-fmk (Enzo Life Sciences); caspase-2 inhibitor z-VD(OMe)VAD(OMe)-fmk, caspase-3/7 inhibitor z-D(OMe)E(Ome)VD(OMe)-fmk, and caspase-8 inhibitor z-IE(OMe)TD(OMe)-fmk (Calbiochem); necrostatin-1, doxycycline (Dox), SP600125, JC-1, propidium iodide, antimycin A, etoposide, and cycloheximide (Sigma Aldrich); CM-H2DCFDA (Molecular Probes); DAPI (VECTOR Laboratories, INC.); nocodazole and LY294002 (Cell Signaling). LzCD95L was described previously (Chen et al., 2010). SMAC mimetic LCL-161 (Active Biochemicals), mitochondrial vitamin E (MVE), which neutralizes mitochondrially generated ROS (Dhanasekaran et al., 2004), was provided by Dr. N. Chandel). Specificity of MVE (coupled to a triphenylphosphonium (TPP) cation moiety) (Dhanasekaran et al., 2004) was established by treating CT26L-pTIP-L3/18 cells with TPP alone. This did not prevent ROS production and DICE (formation of sub G1 DNA) when Dox was added (data not shown).

Doxycycline was added to cells at 0.1 μg/ml. All inhibitors were titered for toxicity using MTS, and the maximally tolerated dose was used for each cell line.

Cell Lines

The ovarian cancer cell line HeyA8, the neuroblastoma cell lines NB7-GFP and NB7-GFP-C8 (NB7 stably expressing caspase-8), the renal cancer cell line CAKI-1, the breast cancer cell lines MDA-MB-231 and MCF-7, and the cervical carcinoma cell line HeLa were cultured in RPMI 1640 medium (Mediatech Inc) containing 10% heat-inactivated foetal bovine serum (FBS) (Sigma-Aldrich) and 1% penicillin/streptomycin (Mediatech Inc). The hepatocellular carcinoma cell line HepG2 was cultured in EMEM medium (ATCC). HT-29 cells stably expressing either a firefly luciferase-specific shRNA or an shRNA targeting MLKL were described elsewhere (Zhao et al., 2012). The murine fibrosarcoma cell line L929 was cultured in MEM medium (ATCC). The colon carcinoma cell lines HCT116, HCT116 *DICER*$^{-/-}$, and HCT116 *TP53*$^{-/-}$ were cultured in McCoy's 5A medium (ATCC). The glioblastoma multiforme cell line T98G and the glioblastoma-astrocytoma cell line U-87 MG were cultured in DMEM medium (Cellgro). The human mammary epithelial cell line MCF10A was cultured in DMEM/F12 medium containing 5% FBS, 1% L-glutamine, 1% penicillin/streptomycin, 1% insulin, 1% epidermal growth factor, 0.5 μg/ml hydrocortisone, and 10 μg/ml gentamycin. The CT26 cell line and human CD95L expressing CT26L cells (a kind gift from Dr. G. Nabel) and the ovarian cancer cell line SKOV3ip1 were cultured as previously described (Chen et al., 2010). Due to the difficulties in detecting small CD95L amounts in MCF-7 cells by Western blotting, MCF-7-CD95L cells engineered to express a low amount of human CD95L as a tracer to determine the extent of CD95L knockdown were used. MCF-7-vec and MCF-7-CD95L cells were generated by infecting MCF-7(-pLNCX2) cells with pLenti-GIII-CMV-RFP-Puro or pLenti-GIII-CMV-RFP-2A-Puro-*FASLG* (accession number BC017502) (ABM) and selected with 3 μg/ml puromycin. NOFs and hTert immortalized NOFs were obtained from Dr. E. Lengyel (University of Chicago) and cultured in DMEM. The surface ovarian epithelial cell line PKOSE-1 (P1) was isolated from *Kras*^{G12D}*Pten*$^{-/-}$ mice as previously described (Mullany et al., 2011). The breast carcinoma cell line MCF-7 transfected with CD95 and a control plasmid (MCF-7-Fas-vector) or CD95 and Bcl-x_L (MCF-7-Fas-Bcl-x_L) were a kind gift from M. Jäättelä (Kopenhagen, Denmark). They were cultured in complete RPMI 1640 medium (Mediatech Inc) containing 250 μg/ml Hygromycin and 200 μg/ml Geneticin.

Knockdown Using Lentiviral shRNAs

Cells were infected with the following MISSION® Lentiviral Transduction Particles (Sigma): pLKO.2-puro Control Transduction Particle coding for a nontargeting (scrambled) shRNA (#SHC002) (CCGGCAACAA GATGAAGAGC ACCAACTCGA GTTGGTGCTC TTCATCTTGT TGTTTTT), shRNA against mRNA NM_001146708.1 (mouse *Fas*) TRCN0000012328 (R28: CCGGGTGTTC TCTTTGCCAG CAAATCTCGA GATTTGCTGG CAAAGAGAAC ACTTTTT), shRNAs against mRNA NM_000043 (Homo sapiens *FAS*) TRCN0000218492 (R2: GTACCGGCTA TCATCCTCAA GGACATTACT CGAGTAATGT CCTTGAGGAT GATAGTTTTTTG) and TRCN0000038696 (R6: CCGGGTGCAG ATGTAAACCA AACTTCTCGA GAAGTTTGGT TTACATCTGC ACTTTTTG), and three different shRNAs against mRNA NM_000639 (Homo sapiens *FASLG*), TRCN0000058998 (L1: CCGGGCATCA TCTTTGGAGA AGCAACTCGA GTTGCTTCTC CAAAGATGAT GCTTTTTG), TRCN0000059000 (L3: CCGGACTGGG CTGTACTTTG TATATCTCGA GATATACAAA GTACAGCCCA GTTTTTTG), and TRCN0000059001 (L4: CCGGGCAGTG TTCAATCTTA CCAGTCTCGA GACTGGTAAG ATTGAACACT GCTTTTTG) according to the manufacturer's instructions. In brief, 50,000 cells seeded in 6 well plates were infected with each lentivirus at a M.O.I. of 3 in the presence of 8 μg/ml polybrene. Cells were cultured in selection medium containing 3 μg/ml of puromycin for two days (except for HepG2 cells, which only required 2 μg/ml puromycin for selection). In all experiments involving puromycin selection, mock infected cells were included and were also treated with puromycin. Cells were only analyzed after all such noninfected cells died within 2-3 days after addition of puromycin. For experiments performed without puromycin selection, 800 T98G cells or 700 HeyA8 cells seeded in 96 well plates were infected with each lentivirus at a M.O.I. of 50 in the presence of 8 μg/ml polybrene. Cells were assayed using Trypan blue staining after 5-8 days.

Transfection with siRNAs

0.2 - 0.5 x 10^6 cells were seeded in 6 well plates one day prior to transfection. Cells were transfected with 5 or 100 nM of a SMART pool of 4 mammalian nontargeting siRNAs, the On-target siRNA SMART pool against human CD95L or 50 nM of the individual oligonucleotides of the SMART pool, (siRNA #1 (siL1) target sequence: UACCAGUGCUGAUCAUUUA; siRNA #2 (siL2) target sequence: CAACGUAUCUGAGCUCUCU; siRNA #3 (siL3) target sequence: GCCCUUCAAUUACCCAUAU; siRNA #4 (siL4) target sequence: GGAAAGUGGCCCAUUUAAC), or siRNA #3 mutant (siL3mut; target sequence: GGACUUCAAUUAGACAUCU) (Dharmacon RNATechnology) using Lipofectamine 2000 (Invitrogen). Alternatively, two mouse CD95L specific On-target siRNAs were used (siRNA #12 (siL12) target sequence: CAACAUAUCUCAACUCUCU; siRNA #13 (siL13) target sequence: GGAAUGGGAAGACACAUAU. 48 or 72 hours post-transfection, cells were trypsinized and CD95L knockdown was monitored by Western blotting. To assess functional effects of CD95L knockdown, and if not otherwise indicated, cells were sequentially transfected on days 0, 3, and 5. Cell death was quantified at day 7 (**Figure 1D**) or on days 0, 4, and 7 and cell death and or growth inhibition was quantified at day 9 (**Figure 1F**).

Real-time PCR

Total RNA was extracted using QIAZOL Lysis reagent (QIAGEN), and 1 μg of total RNA was used to generate cDNA using the High-Capacity cDNA ReverseTranscription Kit (Applied Biosystems). cDNAs were quantified using specific primers from Applied Biosystems for *GAPDH* (Hs00266705_g1), *CD95* (Hs00163653_m1), *RNU6B* (TM:001093), hsa-miR-21 (TM:000397), and hsa-miR-34a (TM:000426).

Cell Size Measurements

Cell size was determined using Flow Jo v. 8.8.4 by setting two (arbitrary but not overlapping) gates representing either normal sized cells or enlarged cells in forward-side scatters of only live cells and applying the gates to all samples. The percentage of cells in either gate was quantified, and the standard deviation for each sample was determined using Student's t-test. To determine whether DICE is cell autonomous, HepG2 cells were infected with pTIG-L3 and after 2 days, cells were treated with Dox for 3 days or left untreated. Cell size was analyzed as described above by gating on GFP negative and positive populations.

Proliferation Assay (SRB)

To study the proliferation of each cell line upon knockdown of CD95 or CD95L, the CytoScan SRB Assay kit (G Biosciences), which quantifies total protein content of cells, was used. Equal numbers of cells were seeded in triplicate in 96 well plates. After incubation for 1-5 days, cells were fixed with the reagent provided with the kit and stained with Sulforhodamine B. Plates were washed, and the remaining dye was solubilized with SRB solubilization buffer. Plates were measured at OD 540 using an iMark Microplate Reader (Biorad).

Cell Growth/Survival Assay

To measure cell viability of cells after knockdown of either CD95 or CD95L, cells were seeded in 96 well plates with or without Dox and/or various inhibitors and incubated at 37°C. Cell viability was determined in triplicate at various time points using the MTS assay according to the manufacturer's instructions (Promega). Plates were measured at OD 490 using an iMark Microplate Reader (Biorad). Data are represented as means ± S.D.

Cell Death Assay (DNA fragmentation)

10,000 cells/well were plated with or without Dox, and plates were incubated at 37°C for 1-5 days. Both dead and live cells were collected for the assay. The total cell pellet was resuspended in Nicoletti buffer (0.1% sodium citrate, pH 7.4, 0.05% Triton X-100, 50 μg/ml propidium iodide). After four hours in the dark at 4°C, fragmented DNA (% sub G1 nuclei) was quantified by flow cytometry (Beckman Coulter).

Western Blot Analysis

Cell lysates were obtained by lysing cells with RIPA lysis buffer (1% SDS, 1% Triton X-100, 1% deoxycholic acid) and quantified using the DC Protein Assay kit (Bio-Rad). Proteins (25-50 μg) in lysates were resolved on 12% SDS-PAGE gels and transferred to nitrocellulose membranes (Protran, Whatman). The membranes were

blocked with 5% non-fat dry milk in 0.1% TBS/Tween-20 (Actin and mouse CD95) or 2% BSA-TBST (human CD95 and human CD95L) and incubated in primary antibodies diluted in blocking solution at 4°C overnight. After incubation with secondary antibodies, detection was performed using the ECL method (Amersham Pharmacia Biotech) and developed using a chemiluminescence imager, G:BOX Chemi XT4 (Synoptics). Quantification of band intensities was performed using GeneTool (Syngene). To detect CD95 in mouse liver, extracts were prepared as previously described (Chen et al., 2010). The final concentration of the primary antibodies in their respective blocking solutions were as follows: Actin (0.4 μg/ml), human CD95L (1 μg/ml), human CD95 (1 μg/ml), and mouse CD95 (1 μg/ml).

ROS and Mitochondrial Transmembrane Potential Measurements

Inside cells, CM-H2DCFDA is cleaved by esterases forming DCFH, which is oxidized to the fluorescent compound DCF by ROS. To measure intracellular ROS production following treatment with Dox for 1–5 days, cells were loaded with 10 μM DCFH-DA for 30 minutes at 37°C. Cells were washed three times with PBS, and ROS was quantified using a FACS flow cytometer (Beckman Coulter). Mitochondrial membrane integrity was assessed by measuring the potential gradient ($\Delta\Psi_m$) across the mitochondrial membrane using the lipophilic, cationic fluorescent dye JC-1 (Sigma). Cells were incubated in 2 μg/ml JC-1 in medium for 30 minutes at 37ºC. After washing twice with PBS, cells were trypsinized, and fluorescence was immediately measured by flow cytometry.

Caspase-2 Activity Measurement

After Dox treatment of cells, caspase-2 activity was measured in situ using FAM-VDVAD-FMK (ImmunoChemistry Technologies, LLC) according to the manufacturer's instructions. Briefly, cells were harvested, the pellet was resuspended in 290 μl of medium, and 10 μl of 30x FAM-VDVAD-FMK was added. Cells were incubated 1 hour at 37°C, washed with PBS, and resuspended in 300 μl of medium. Cells were kept on ice protected from light and immediately analyzed by flow cytometry.

Surface CD95L Staining

Adherent cells were first detached by trypsinization and counted. 200,000 cells were incubated with 1 μg of anti-CD95L Ab or isotype control Ab in 2% BSA/PBS on ice for 30 minutes. Cells were washed twice with cold 2% BSA/PBS and incubated with mouse IgG-RPE secondary Ab at a dilution of 1:200 in 2% BSA/PBS on ice. After 30 minutes, cells were washed, and CD95L surface staining was assessed by flow cytometry analysis.

Immunofluorescence Microscopy

Cells were fixed with 4% paraformaldehyde (PFA) for 10 minutes, permeabilized with PBS containing 1% Triton X-100 for 10 minutes, and blocked for 1 hour in PBS containing 0.1% Triton X-100, 3% BSA prior to incubation with primary antibodies. Secondary antibodies were FITC-conjugated goat IgG (Southern Biotechnology Associates, INC). Slides were mounted with VECTASHIELD mounting medium containing DAPI (VECTOR Laboratories, INC). For DAPI staining, cells were detached, fixed in 4% PFA, and then resuspended in PBS. A small drop of cell suspension was applied with VECTASHIELD mounting medium containing DAPI onto a coverslip.

Time-Lapse Video Microscopy

Cells were cultured in glass-bottomed dishes (MatTek Corporation) in DMEM + 10% FCS. Treated cells were monitored using a BioStation IM microscope equipped with a thermostatic chamber (Nikon Instruments Inc). Images were acquired at 40x magnification every 30 minutes or every hour over a period of 96 hours. Videos were analyzed with BioStation software and re-run at 4x real time speed to give an indication of cell motility. For T98G-pTIP-L3 cells, HCT116-pTIP-R6 cells, and CT26L-pTIP-L3/18-22 cells, the time-lapse videos obtained (54 for T98G cells, 61 for HCT116 cells, 30 for clone #18 and 30 for clone #22) were separated into 3 sets (for T98G and HCT116 cells) or 6 sets (for CT26L cells), and the cells that died without rounding-up, the cells that died after rounding up, and the cells that died after trying to divide were counted. For CT26L-pTIP-L3/18 cells, time-lapse videos (30 for –zVAD-fmk and 20 for +zVAD-fmk) were separated into sets (6 for –zVAD-fmk and 4 for +zVAD-fmk) of 5 each, and the cells that died with or without blebbing (as shown in **Figure S5A**) were counted. Percentages of cells are shown with SD (n indicates the total number of events

counted). In all cases, at least 50 cells were analyzed.

Electron Microscopy

Cells were grown in DMEM + 10% FCS and treated with Dox. Cells were rinsed with PBS and fixed in 2.5% glutaraldehyde in 0.1 M sodium cacodylate (pH 7.3) for 1 hour on ice. Cells were then rinsed and postfixed in 1% OsO_4 for 1 hour. Cells were rinsed, dehydrated, and embedded in plastic. Specimens were sectioned, stained, and photographed using an FEI Tecnai Spirit G2 120kV transmission electron microscope (TEM).

Comet Assay

Alkaline comet assays were performed using the Trevigen's Comet Assay kit (4250-050-k) according to the manufacturer's instructions. DNA was stained with SYBR Green, and slides were photographed using a Zeiss Axiovert 200 M microscope equipped with a cooled Retiga 2000R CCD (QImaging). Tail moments were analyzed using Tritek CometScore Freeware. 100-150 cells/sample were analyzed.

Generation of Single Cell Ovarian Cancer Clones from Mutant Mice

Ascites was taken from a mouse with ovarian cancer and cultivated in DMEM-F12 media (Gibco), 10% FBS, 1% Insulin-Transferrin-Selenium (Gibco), 1% Glutamine, and 1% Penicillin-Streptomycin. Fresh medium was added every 2 to 3 days, and cells were passaged when subconfluent. After at least 15 passages, single cell cloning was performed at 0.5 cells/well in 200 µl in 96 well plates. Cells were expanded by trypsinization and replated.

shRNA Screen

CT26L-pTIG-L3 cells were generated as described above. The top 10% green cells were sorted using Beckman Coulter's Moflo sorter. Single clones were isolated by limited dilution and selected based on their ability to completely die upon knockdown of CD95L. One such clone, CT26L-pTIG-L3/54, which died completely upon addition of Dox (data not shown), was used to perform two screens (A and B) using the MISSION LentiPlex™ Mouse Pooled shRNA Library (Sigma). In screen A, the ten shRNA virus pools with about 7,500 shRNAs each were combined and 30 million cells were infected (**Figure S8B**). 2 days after infection, puromycin was added, and cells were selected for 7 days. In screen B, 10 individual dishes with 3 million cells each were individually infected with one of ten shRNA pools that made up the entire library. 2 days after infection, puromycin was added (**Figure S8C**). After 7 days of selection, the 10 dishes were combined. Cells were taken as uninduced controls from each screen, and 100 µg/ml Dox was added to both screen A and B. Genomic DNA was isolated after 4 days of Dox treatment and subjected to one round of deep sequencing by Sigma based on a modified Pooled shRNA screening method described elsewhere (Possemato et al., 2011). In short, genomic DNA was isolated from cells by digestion with proteinase K followed by isopropanol precipitation. To amplify the shRNAs encoded in the genomic DNA, PCR was performed for 33 cycles at an annealing temperature of 66 °C using 2–6 µg of genomic DNA, using specific primers. Forward primers contained unique 2-nucleotide barcodes so that PCR products obtained from different samples could be sequenced together. After purification, the PCR products from each sample were quantified by Ethidium bromide staining, pooled at equal proportions, and analyzed by high-throughput sequencing (Illumina) using specific primers. Cluster generation and sequencing were performed according to the cluster generation manual and sequencing manual from Illumina (Cluster Station User Guide and Genome Analyzer Operations Guide). Base calls were generated using Casava 1.8.2 (Illumina). The resulting sequences were trimmed and demultiplexed using custom software developed by Cofactor Genomics. Alignments to the known shRNA sequences were performed with Novoalign 2.07.18 and then counted to determine raw expression levels. Absolute expression counts were also scaled and normalized linearly by multiplying each sample's coverage by the total reads of the lowest read-count sample divided by the respective sample's total reads. This normalized expression data was the basis for the expression comparison. The comparative expression approach stepped through each gene and compared every possible pairing of samples and generated a log2(A/B), where A and B were the normalized average coverage of each sample, A and B. Genes with coverage below 10X were not considered in the comparative expression pipeline (but were retained in the absolute count data) in order to avoid a high percentage of false positives observed in low level expression data. shRNAs were removed with a combined number of reads in the control sample and

Dox treated sample of less than 100. Only genes were considered that were either enriched or underrepresented (more than 2-fold) in both screens. Only genes were considered that were targeted by two or more shRNAs.

Mouse Genotyping

To determine genotypes of mice, DNA was isolated from mouse tails using a DirectPCR Lysis Reagent (Tail) (Viagen Biotech Inc.) with a final concentration of 0.2 mg/ml Proteinase K (Sigma-Aldrich). Tail digestion was performed according to the manufacturer's protocol. The primer sequences used are listed in **Table S5**. Primers were designed using Primer3 (http://frodo.wi.mit.edu/). Primers were synthesized by Integrated DNA Technologies. The optimal melting temperature was determined by gradient PCR. PCR reactions were performed with the Choice Tag™ Blue DNA Polymerase Mastermix (Denville Scientific Inc.) according to the manufacturer's instructions. Primers were added at 10 or 25 nM final concentration. 1 ml of DNA tail lysate was added as template to the PCR reaction mix. PCR reactions were performed on a GeneAmp PCR System 9700 (Applied Biosystems) or a MJ Mini Personal Thermal Cycler (BioRad). The PCR products were analyzed on a 1 to 2% Agarose 1xTAE gels stained with Ethidium bromide. To genotype single cell clones grown on 96 well plates, half of the trypsinized clones were used for expansion and were plated onto a 6 well plate. The other half of the cells was resuspended in one volume of PBS and lysed with an equal amount of Tail DirectPCR Lysis Reagent (Tail) (Viagen Biotech Inc.) with a final concentration of 0.4 mg/ml Proteinase K. Cells were incubated overnight at 56°C, and Proteinase K activity was inactivated by incubating the samples at 85°C for 45 minutes. 1 to 10 ml were used as template for PCR reactions.

Immunohistochemistry of Ovaries and Livers

Ovaries from female mice of the various genotypes were excised after about 80 days and photographed using an iPhone 4 digital camera. Ovaries were fixed in 10% normal buffered formalin for approximately 24 hours before they were paraffin embedded. The Mouse Histology and Pathology Laboratory (MHPL) of Northwestern University performed the processing of the ovaian cancer tissue samples as well as the Hematoxilin and Eosin (H&E) staining. Other stainings and IHC analyses were perfromed by The Lurie Cancer Center's Pathology Core Facility (PCF). For the cytokeratin 8/18 staining slice thickness was 4 μm. Sections were analyzed by an expert pathologist. For immunohistochemistry, tissue sections were deparaffinized and rehydrated through xylenes and serial dilutions of EtOH to distilled water. CK8/18 staining was performed using standard immunohistochemical techniques. Antigen was recovered using a sodium citrate buffer pH 6.0 in a pressure cooker. The monoclonal anti CK8/18 antibody (University of Iowa (1:20, TROMA-1, Developmental Studies Hybridoma Bank, DSHB)) was incubated for 30 minutes followed by anti-rat secondary Ab (K0690-biotinylated link Universal, Dako) incubation for 30 minutes. Dako LSAB system HRP labeled streptavidin was used as the detection system for 15 minutes. Generation of mice with tissue specific deletion of CD95 in the liver (*CD95*$^{loxP/loxP}$*Albumin(Alb)-Cre*) and induction of liver cancer by injection of DEN was described previously (Chen et al., 2010). Livers of four wild-type and two randomly selected *CD95*$^{loxP/loxP}$*Alb-Cre* mice were stained for CD95 expression using two different anti-CD95 antibodies: Rabbit IgG (500 μg/ml) (LifeScience Bio, Cat #LS-B6851) and mouse IgG, clone: 13/FAS (250 μg/ml) (BD Biosciences, Cat #610197). To stain with the rabbit antibody, 5 μm sections were incubated in antigen retrieval buffer (DAKO, S1699) and heated in a steamer at over 97ºC for 20 minutes. Antibody (1:50 or 1:100) was applied on tissue sections for 1 hour at room temperature. To stain with the mouse mAb, sections were treated with 1% SDS in PBS for 5 minutes at room temperature. Antibody (1:40 or 1:80) was applied on tissue sections for 1 hour at room temperature. Following a TBS wash, tissue sections were incubated with either biotinylated anti-rabbit IgG (1:200, BA-1000, Vector Laboratories) or with biotinylated anti-mouse IgG (1:100, BA-2001, Vector Laboratories) for 30 minutes at room temperature. The antigen-antibody binding was detected by Elite kit (PK-6100, Vector Laboratories) and DAB (DAKO, K3468) system. Mouse IgG blocking reagent was used for mouse tissues.

Morphogenic Analysis.

H&E, C8/18, and CD95 staining of mouse ovary and liver was evaluated after scanning the slides with NanoZoomer 2.0-HT: C9600-13 scanner (Hamamatsu Photonics). Morphometric parameters were measured by

annotation tools in NanoZoomer view software (Hamamatsu Photonics). Examples of outlined areas are shown in **Figure S9D**. Surface area of total ovary, surface area of borderline serous epithelial tumor (CK8/18 positive), and area of hemorrhagic cystic lesions in both left and right ovaries were quantified. Similarly, mouse liver hyperplastic nodules measurements were taken. The H-score system (Budwit-Novotny et al., 1986) (3 x percentage of strongly staining cells + 2 x percentage of moderately staining cells + percentage of weakly staining cells, giving a range of 0 to 300) was used for evaluation of CD95 staining in benign and tumor regions by a single observer (V.P.). To normalize the H-score for different sizes of analyzed nodules, the following formula was used: Sum of normalized H-score of all nodules (Normalized H-score = (area of nodule in mm^2/total area of all nodules in mm^2) * H-score of nodule)).

Statistical Analysis

Experiments were performed in triplicate. The results were expressed as mean + SD and analyzed by the Student's two-tailed t-test or by ANOVA (Statplus v.5.8). Statistical significance was defined as $p < 0.05$.

Supplementary References

Bianco, C., Tortora, G., Basolo, F., Fiore, L., Fontanini, G., Merlo, G., Salomon, D., Bianco, A., and Ciardiello, F. (1994). Effects of mutant p53 genes on transformation of human mammary epithelial-cells. Int J Oncol *4*, 1077-1082.

Budwit-Novotny, D.A., McCarty, K.S., Cox, E.B., Soper, J.T., Mutch, D.G., Creasman, W.T., Flowers, J.L., and McCarty, K.S., Jr. (1986). Immunohistochemical analyses of estrogen receptor in endometrial adenocarcinoma using a monoclonal antibody. Cancer Res *46*, 5419-5425.

Bunz, F., Dutriaux, A., Lengauer, C., Waldman, T., Zhou, S., Brown, J.P., Sedivy, J.M., Kinzler, K.W., and Vogelstein, B. (1998). Requirement for p53 and p21 to sustain G2 arrest after DNA damage. Science *282*, 1497-1501.

Casagrande, F., Bacqueville, D., Pillaire, M.J., Malecaze, F., Manenti, S., Breton-Douillon, M., and Darbon, J.M. (1998). G1 phase arrest by the phosphatidylinositol 3-kinase inhibitor LY 294002 is correlated to up-regulation of p27Kip1 and inhibition of G1 CDKs in choroidal melanoma cells. FEBS Lett *422*, 385-390.

Chen, L., Park, S.M., Tumanov, A.V., Hau, A., Sawada, K., Feig, C., Turner, J.R., Fu, Y.X., Romero, I.L., Lengyel, E.*, et al*. (2010). CD95 promotes tumour growth. Nature *465*, 492-496.

Dhanasekaran, A., Kotamraju, S., Kalivendi, S.V., Matsunaga, T., Shang, T., Keszler, A., Joseph, J., and Kalyanaraman, B. (2004). Supplementation of endothelial cells with mitochondria-targeted antioxidants inhibit peroxide-induced mitochondrial iron uptake, oxidative damage, and apoptosis. J Biol Chem *279*, 37575-37587.

Kimchi-Sarfaty, C., Oh, J.M., Kim, I.W., Sauna, Z.E., Calcagno, A.M., Ambudkar, S.V., and Gottesman, M.M. (2007). A "silent" polymorphism in the MDR1 gene changes substrate specificity. Science *315*, 525-528.

Liu, X., Yang, J.M., Zhang, S.S., Liu, X.Y., and Liu, D.X. (2010). Induction of cell cycle arrest at G1 and S phases and cAMP-dependent differentiation in C6 glioma by low concentration of cycloheximide. BMC Cancer *10*, 684.

Luo, J.L., Maeda, S., Hsu, L.C., Yagita, H., and Karin, M. (2004). Inhibition of NF-kappaB in cancer cells converts inflammation- induced tumor growth mediated by TNFalpha to TRAIL-mediated tumor regression. Cancer Cell *6*, 297-305.

Modesitt, S.C., Ramirez, P., Zu, Z., Bodurka-Bevers, D., Gershenson, D., and Wolf, J.K. (2001). In vitro and in vivo adenovirus-mediated p53 and p16 tumor suppressor therapy in ovarian cancer. Clin Cancer Res *7*, 1765-1772.

Mullany, L.K., Fan, H.Y., Liu, Z., White, L.D., Marshall, A., Gunaratne, P., Anderson, M.L., Creighton, C.J., Xin, L., Deavers, M.*, et al*. (2011). Molecular and functional characteristics of ovarian surface epithelial cells transformed by KrasG12D and loss of Pten in a mouse model in vivo. Oncogene *30*, 3522-3536.

O'Connor, P.M., Jackman, J., Bae, I., Myers, T.G., Fan, S., Mutoh, M., Scudiero, D.A., Monks, A., Sausville, E.A., Weinstein, J.N.*, et al*. (1997). Characterization of the p53 tumor suppressor pathway in cell lines of

the National Cancer Institute anticancer drug screen and correlations with the growth-inhibitory potency of 123 anticancer agents. Cancer Res *57*, 4285-4300.

Possemato, R., Marks, K.M., Shaul, Y.D., Pacold, M.E., Kim, D., Birsoy, K., Sethumadhavan, S., Woo, H.K., Jang, H.G., Jha, A.K., *et al*. (2011). Functional genomics reveal that the serine synthesis pathway is essential in breast cancer. Nature *476*, 346-350.

Van Meir, E.G., Kikuchi, T., Tada, M., Li, H., Diserens, A.C., Wojcik, B.E., Huang, H.J., Friedmann, T., de Tribolet, N., and Cavenee, W.K. (1994). Analysis of the p53 gene and its expression in human glioblastoma cells. Cancer Res *54*, 649-652.

Vollmer, C.M., Ribas, A., Butterfield, L.H., Dissette, V.B., Andrews, K.J., Eilber, F.C., Montejo, L.D., Chen, A.Y., Hu, B., Glaspy, J.A., *et al*. (1999). p53 selective and nonselective replication of an E1B-deleted adenovirus in hepatocellular carcinoma. Cancer Res *59*, 4369-4374.

Wischhusen, J., Naumann, U., Ohgaki, H., Rastinejad, F., and Weller, M. (2003). CP-31398, a novel p53-stabilizing agent, induces p53-dependent and p53-independent glioma cell death. Oncogene *22*, 8233-8245.

Zhao, J., Jitkaew, S., Cai, Z., Choksi, S., Li, Q., Luo, J., and Liu, Z.G. (2012). Mixed lineage kinase domain-like is a key receptor interacting protein 3 downstream component of TNF-induced necrosis. Proc Natl Acad Sci U S A *109*, 5322-5327.